

## Article

# Estimating Errors in Sizing LID Device and Overflow Prediction Using the Intensity-Duration-Frequency Method

Shuangcheng Tang, Qing Xu, Zhonghua Jia \*, Wan Luo and Zhengxiao Shao

School of Hydraulic Energy and Power Engineering, Yangzhou University, Yangzhou 225009, China

\* Correspondence: jiazh@yzu.edu.cn; Tel.: +0514-8797-1315

Received: 19 July 2019; Accepted: 3 September 2019; Published: 5 September 2019



**Abstract:** Low impact development (LID) devices or green infrastructures have been advocated for urban stormwater management worldwide. Currently, the design and evaluation of LID devices adopt the Intensity-Duration-Frequency (IDF) method, which employs the average rainfall intensity. However, due to variations of rainfall intensity during a storm event, using average rainfall intensity may generate certain errors when designing a LID device. This paper presents an analytical study to calculate the magnitude of such errors with respect to LID device design and associated device performance evaluation. The normal distribution rainfall (NDR) with different standard deviations was employed to represent realistic rainfall processes. Compared with NDR method, the error in sizing the LID device was determined using the IDF method. Moreover, the overflow difference calculated using the IDF method was evaluated. We employed a programmed hydrological model to simulate different design scenarios. Using storm data from 31 regions with different climatic conditions in continental China, the results showed that different rainfall distributions (as represented by standard deviations ( $\sigma$ ) of 5, 3, and 2) have little influence on the design depth of LID devices in most regions. The relative difference in design depth using IDF method was less than 1.00% in humid areas,  $-0.61\%$  to  $3.97\%$  in semi-humid areas, and the significant error was  $46.13\%$  in arid areas. The maximum absolute difference in design depth resulting from the IDF method was 2.8 cm. For a LID device designed for storms with a 2-year recurrence interval, when meeting for the 5-year storm, the relative differences in calculated overflow volume using IDF method ranged from  $19.8\%$  to  $95.3\%$ , while those for the 20-year storm ranged from  $7.4\%$  to  $40.5\%$ . The average relative difference of the estimated overflow volume was  $29.9\%$  under a 5-year storm, and  $12.0\%$  under a 20-year storm. The relative difference in calculated overflow volumes using IDF method showed a decreasing tendency from northwest to southeast. Findings from this study suggest that the existing IDF method is adequate for use in sizing LID devices when the design storm is not usually very intense. However, accurate rainfall process data are required to estimate the overflow volume under large storms.

**Keywords:** LID; rainfall distribution; design depth; overflow volume; hydrological model

## 1. Introduction

To mitigate the negative impact of urbanization on stormwater management, green development concept, such as the Low Impact Development (LID) in the US or the Water Sensitive Urban Design in Australia etc., has been widely advocated to mitigate stormwater runoff, these employ onsite infiltration-storage devices to reduce peak flow rates and total runoff volume [1–4]. In light of the concept, China has issued a sponge city construction plan to increase the resilience of cities in combating adverse weather conditions. Two groups of cities have been chosen as demonstration sites with special funding to build green infrastructures or LID devices to enhance urban storm drainage systems [5,6].

LID stormwater devices or structures are small depressional areas that receive concentrated storm runoff. They are soil and plant-based bioretention devices that remove pollutants through a variety of physical, biological, and chemical treatment processes [7–9]. Since adding LID devices may ease the pressure of urban drainage system, the retention effect of LID devices will be taken into consideration in urban drainage system design in the future [10]. However, the retention effect of a LID device is affected by different storm processes, therefore, it is important to use an appropriate design storm when considering LID device design [11,12]. Currently, the design storm for a LID device usually adopts municipal drainage guidelines where the design storm is represented by its intensity, duration, and frequency (IDF) [13–15]. The IDF method has long been used as a standard approach in designing urban stormwater systems, such as drainage pipe sizing [16,17]. However, when conducting LID design and flow calculation that considers the variable nature of the intensity of rainfall during a storm event, the rainfall intensity of IDF is the average intensity of the storm duration, and its application could lead to certain errors [18]. As the front input parameter, storm process distribution is of vital important for designing LID devices and urban drainage systems [19]. Therefore, when the rainfall distribution is greatly simplified with the IDF method, application of this method for sizing or evaluating the LID device may introduce certain errors. If such errors are within certain limits, the simplified IDF method would be applicable. Otherwise, a more accurate design method should be used.

Storm processes are random events, and their frequency distribution is varied. Cen et al. [20] studied the characteristics of rainfall distribution in four regions and determined that the Chicago rainfall pattern met storm design requirements with respect to a few design parameters. However, the Chicago rainfall pattern was cusp and thin, which was quite different from the actual situation. They also found that rainfall intensity peaks occurred mostly in the front or the middle part of a rainfall event. To accurately portray the storm distribution, the Pearson Type 3 distribution, normal distribution, and exponential distribution are widely used in urban storm drainage design [20–22]. Khatavkar et al. [23] proposed an optimization model for the design of vegetative filter strips where the design storm employed a six-hour storm rainfall hyetograph, which is also the mean rainfall intensity duration. Chin [24] presented a design protocol for sizing a bioretention device where the design storm was obtained from the IDF curves nested within each of the four Natural Resources Conservation Service (NRCS) 24-h hyetographs. At the same time, the impacts of different rainfall distributions on flood control and water-quality control were analyzed, and the results demonstrated that the bioretention device that is designed for water-quality control could also meet flood-control regulation. Furthermore, Kurtz [25] used detailed storm process data and found that a 1-min interval storm provided more accurate hydrologic results than using 5-min interval data.

Several models can simulate rainfall-runoff processes considering LID devices. Info Works and MIKE URBAN are often used for real-time dynamic simulation of rainfall flood in basin level [26,27]. SWMM is the most deeply studied and most mature urban rainfall-runoff-water quality model in the world. SWMM model divides the study area into sub-catchment areas, which is suitable for LID simulation in small areas and the integration effect in large areas [28]. SUSTAIN has integrated various hydrological water quality simulations such as SWMM and embedded in ArcGIS software, which are used for analysis and optimization of LID system [29]. Other studies also discussed the RECHARGE and DRAINMOD for hydrological process modeling of LID devices [30]. This paper mainly studies the influence of rainfall distribution on the design and evaluating the hydrological performance of a single LID device. It is obvious that the distributed hydrological models at the watershed level such as Info Works and MIKE URBAN are not suitable for use. SWMM and SUSTAIN can be employed to imitate the hydrological process of a single LID device, but complex model parameters such as pipe networks and GIS need to be taken into account. Based on the water balance in a LID device, an analytical model is programmed for use in designing a LID device and evaluating the hydrological performance of a LID device.

Currently, most LID designs adopt a regional rational formula that assumes a uniform rainfall intensity distribution during a design storm [31]. LID devices reduce runoff mainly through an onsite infiltration process. In this respect, collected storm runoff is temporarily ponded in the surface storage layer of the LID device and is then overflowed to the city drainage system or via deep percolation to groundwater. An overflow inlet is often installed to divert excessive inflow to the city drainage system during large storm events [32,33]. Therefore, the surface design depth and overflow volume of the LID device are two important parameters that need to be accurately addressed when evaluating the performance of a LID device. The surface depth and the runoff catchment area ratio are the two important design parameters of a LID device [34]. These design parameters are affected by the infiltration capacity of the LID device and the regional rainfall characteristics. For countries with a vast territory, such as China, regional differences in soil type and rainfall characteristics could result in significant errors in the design parameters of LID devices.

To investigate the magnitude of such potential errors, this paper presents an analytical study on the applicability of using the IDF method in LID device design. Here, the normal distribution rainfall (NDR) with different standard deviations was used to represent actual rainfall processes, and errors resulting from using IDF method in the LID design were compared to examine:

- (1) the potential errors in sizing LID device, and
- (2) the difference in estimating overflows under large storms.

## 2. Material and Methods

### 2.1. Study Area and General Water Balance Model for LID Infiltration Device

Under the sponge city construction plan, China has selected two groups of cities to demonstrate the effect of LID construction on urban stormwater management. The demonstrated cities are scattered across the country and have quite different climatic conditions [35]. For example, Shenzhen is located in the humid south and has an annual rainfall of more than 1500 mm, while Guyuan is located in a semi-arid region in the northwest and has an annual rainfall of 400 mm. Due to eventual implementation for the sponge city construction plan throughout the country, we selected 31 provincial capital cities in continental China to analyze the errors of using IDF method on the design of the LID device. Table 1 lists the standard urban storm intensity formula employed with the IDF method as provided by the National Hydrological Agency of China [36]. To provide a common ground for comparison, we selected a set of design parameters from the technical guideline for sponge city construction issued by the Ministry of Housing and Urban-Rural Development [5].

A sketch of the general water balance in a LID device is presented in Figure 1.

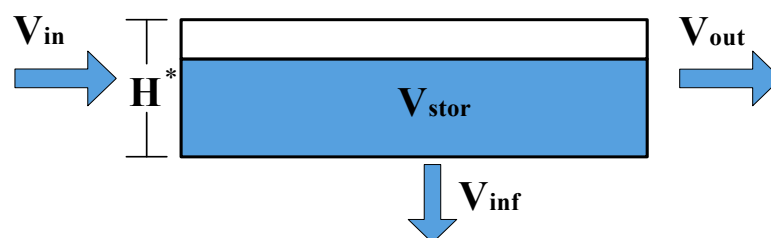


**Figure 1.** Schematic diagram of water balance for LID device ( $H^*$  is the designed depth).

**Table 1.** Standard urban storm intensity formula <sup>a</sup>.

NO.	Provinces and Municipalities	Rainstorm Intensity Formula	NO.	Provinces and Municipalities	Rainstorm Intensity Formula
1	Hefei	$i = \frac{24.927+20.228\lg T_E}{(t+17.008)^{0.863}}$	17	Hohhot	$i = \frac{9.96(1+0.985\lg P)}{(t+5.40)^{0.85}}$
2	Beijing	$i = \frac{10.662+8.842\lg T_E}{(t+7.857)^{0.679}}$	18	Yinchuan	$q = \frac{242(1+0.83\lg P)}{t^{0.477}}$
3	Xiamen	$q = \frac{1085.020(1+0.581\lg T_E)}{(t+2.954)^{0.559}}$	19	Xining	$q = \frac{308(1+1.39\lg P)}{t^{0.58}}$
4	Lanzhou	$i = \frac{18.260+18.984\lg T_E}{(t+14.317)^{1.066}}$	20	Jinan	$q = \frac{4700(1+0.753\lg P)}{(t+17.5)^{0.898}}$
5	Guangzhou	$i = \frac{11.163+6.646\lg T_E}{(t+5.033)^{0.625}}$	21	Taiyuan	$q = \frac{1446.22(1+0.867\lg T)}{(t+5)^{0.796}}$
6	Nanning	$i = \frac{32.287+18.194\lg T_E}{(t+18.880)^{0.851}}$	22	Xi'an	$i = \frac{37.603+50.124\lg T_E}{(t+30.177)^{1.078}}$
7	Guiyang	$i = \frac{6.853+1.195\lg T_E}{(t+5.168)^{0.601}}$	23	Shanghai	$i = \frac{9.4500+6.7932\lg T_E}{(t+5.54)^{0.6514}}$
8	Shijiazhuang	$i = \frac{10.785+10.176\lg T_E}{(t+7.876)^{0.741}}$	24	Chengdu	$i = \frac{20.154+13.371\lg T_E}{(t+18.768)^{0.784}}$
9	Zhengzhou	$q = \frac{3073(1+0.892\lg P)}{(t+15.1)^{0.824}}$	25	Tianjin	$i = \frac{49.586+39.846\lg T_E}{(t+25.334)^{1.012}}$
10	Harbin	$q = \frac{2889(1+0.9\lg P)}{(t+10)^{0.88}}$	26	Urumqi	$q = \frac{195(1+0.82\lg P)}{(t+7.8)^{0.63}}$
11	Wuhan	$i = \frac{5.359+3.996\lg T_E}{(t+2.834)^{0.510}}$	27	Kunming	$i = \frac{8.918+6.183\lg T_E}{(t+10.247)^{0.649}}$
12	Changsha	$i = \frac{24.904+18.632\lg T_E}{(t+19.801)^{0.863}}$	28	Hangzhou	$i = \frac{10.600+7.736\lg T_E}{(t+6.403)^{0.686}}$
13	Changchun	$i = \frac{6.337+5.70\lg T_E}{(t+4.367)^{0.633}}$	29	Chongqing	$q = \frac{2822(1+0.775\lg P)}{(t+12.8P^{0.076})^{0.77}}$
14	Nanjing	$i = \frac{16.060+11.914\lg T_E}{(t+13.228)^{0.775}}$	30	Haikou	$q = \frac{2338(1+0.4\lg P)}{(t+9)^{0.65}}$
15	Nanchang	$q = \frac{1386(1+0.69\lg P)}{(t+1.4)^{0.64}}$	31	Lhasa	$i = \frac{5.7203+6.6653\lg T_E}{(t+6.2892)^{0.8643}}$
16	Shenyang	$i = \frac{11.522+9.348\lg P_E}{(t+8.196)^{0.738}}$			

a: Adopted from the National Urban Storm Intensity Formula Catalogue [36]. Where  $i$  is the rainfall intensity, mm/min;  $q$  is the rainfall intensity per hectare, L/(s·hm<sup>2</sup>);  $P$  and  $T_E$  represent the rainfall frequency, year;  $t$  is rainfall duration, minute.

If evaporation during rainfall is ignored, the water balance can be expressed as in Equation (1),

$$V_{in} = V_{inf} + V_{stor} + V_{out} \quad (1)$$

where  $V_{in}$ ,  $V_{inf}$ ,  $V_{stor}$ , and  $V_{out}$  are volumes of inflow, infiltration, storage, and outflow, respectively.

Apparently, flow retention and overflow volumes are directly related to the device size and soil infiltration capacity. When the IDF method is used in LID device design, the infiltration rate is treated as a constant, although the initial infiltration rates may be much higher when soils are dry. The procedures used to size and evaluate the LID device under different situations are presented in the following sections.

## 2.2. LID Device Sizing and Outflow Estimation with Different Methods

### 2.2.1. Normal Distribution to Represent Realistic Rainfall Processes

In general, rainfall distribution is random, and the rainfall intensity is often smaller at the beginning and end of a rainfall period. Different rainfall processes can be represented using the normal distribution (NDR) with various standard deviations. The normal distribution function is expressed as,

$$f(x) = \frac{1}{\sigma\sqrt{2\pi}} e^{-\frac{(x-\mu)^2}{2\sigma^2}} \quad (2)$$

where  $\mu$  is the mean of the distribution,  $\sigma$  is the standard deviation. Different rainfall distributions are represented with different standard deviations ( $\sigma$ ), and smaller values of standard deviation ( $\sigma$ ) indicate more intense rainfall events.

Since nearly all data lie within 6 standard deviations of the mean in a normal distribution,  $\sigma$  of 2, 3, and 5 are selected to represent different rainfall processes. Keeping the total rainfall amount constant, the normally distributed rainfall intensity can be obtained through the following transformation,

$$t = x \times \frac{T}{12} + \frac{T}{2} \text{ and } I = k \times \frac{1}{\sigma \sqrt{2\pi}} e^{-72 \times \left(\frac{2t-T}{2\sigma T}\right)^2} \times (12I_r) \quad (3)$$

where  $t$  is the time of duration,  $x$  is the independent variable of the normal distribution from  $-6$  to  $6$ ,  $T$  is storm duration,  $I$  is the normal distribution rainfall intensity, and  $I_r$  is the average rainfall intensity used in the IDF method, and  $k$  is a correction factor used for adjusting the rainfall intensity bell curve to match the total rainfall amount (for example, 3 standard deviations account for 99.73%,  $k = 1/0.9973$ ).

When the rainfall intensity is expressed using the NDR, different standard deviations ( $\sigma$ ) represent different rainfall distributions with variable peak values. To examine the differences in NDR intensity with different standard deviations from the average rainfall intensity using the IDF method, the ratio between the rainfall intensity with the NDR method and that of the IDF was calculated and presented in Figure 2. When  $\sigma = 2$ , the ratio between the NDR and IDF has the smallest value of 0.03 at both ends of the duration, and the largest ratio is 2.40 in the middle of the design rainfall duration, when  $\sigma = 3$ , the smallest ratio is 0.23, and the largest ratio is 1.67, when  $\sigma = 5$ , the ratio ranges from 0.61 to 1.64. A larger value of  $\sigma$  indicates flatter rainfall distribution pattern or near-average rainfall intensity that can be well represented by the IDF method.

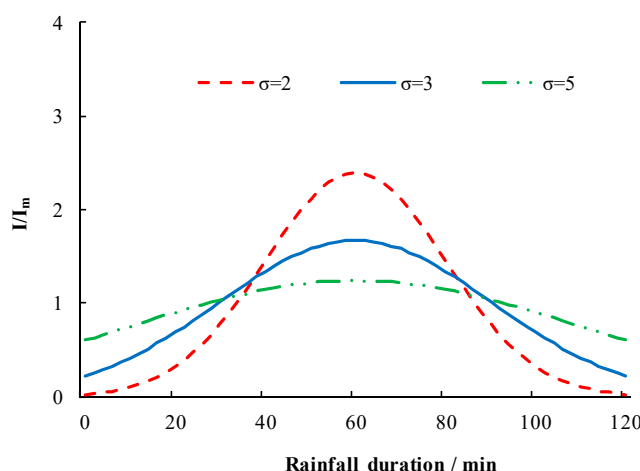


**Figure 2.** Ratio of rainfall intensity with NDR of different standard deviations over IDF.

The infiltration rate can be calculated with the Green-Ampt equation as:

$$k = \frac{A}{F} + K_s \quad (4)$$

where  $K_s$  is the saturated hydraulic conductivity of the rain garden soil, m/d,  $F$  is cumulative-infiltration volume, m, and  $A$  is a constant value relating to soil properties and soil water content that can be estimated as:

$$A = \frac{bS^2}{K_s} \quad (5)$$

where  $b$  is a constant between 0.5 and  $\pi/4$  (normally taken as 0.55),  $S$  is the hygroscopic rate of the soil, which is closely related to the moisture content, degree of compaction, and clay content [37].

### 2.2.2. IDF Method

For current method that uses an IDF rainfall distribution, the infiltration process is assumed to be stable with a unit hydraulic gradient. The inflow volume to the LID device can be calculated as:

$$V_{in} = (I_r \times s \times \eta + I_r) \times T \times A_{LID} \quad (6)$$

where  $I_r$  represents the design rainfall intensity (mm/min),  $s$  represents the catchment area ratio,  $\eta$  is the runoff coefficient,  $T$  is the rainfall duration (min), and  $A_{LID}$  is the surface area of the LID device (m<sup>2</sup>).

If the design storm is just enough to fill up the storage space of a LID device and no outflow occurs, the design depth of the LID device ( $H^*$ ) is:

$$H^* = (I_r \times s \times \eta + I_r - k) \times T \quad (7)$$

where  $k$  is the infiltration capacity of soil (m/d), it can be approximated as the saturated hydraulic conductivity of the soil.

For storms that exceed the design level, they may produce overflow from the device, and the overflow volume can be calculated as:

$$W_{out} = (T - t_0') \times [I_r \times (\eta s + 1) - k] \quad (8)$$

where  $W_{out}$  is the overflow volume from the LID device, and  $t_0'$  is the overflow starting time that can be estimated as:

$$t_0' = H / (I_r \times s \times \eta + I_r - k) \quad (9)$$

### 2.2.3. Computing Procedure and Programming

When both rainfall and infiltration processes vary with time, the water balance of a LID device can be expressed as:

$$A_{LID} \times \frac{dH}{dt} = Q_{in} - Q_{out} - Q_{inf} \quad (10)$$

where  $H$  is the ponding depth (m),  $t$  is time (min), and  $Q_{in}$ ,  $Q_{out}$ ,  $Q_{inf}$  are the inflow and outflow and infiltration volumes (m<sup>3</sup>), respectively.

The inflow and infiltration volumes during a certain time period can be expressed as:

$$Q_{in} = \int_0^t (\eta \times s + 1) A_{LID} \times I dt \quad (11)$$

$$Q_{inf} = \int_0^t k \times A_{LID} dt \quad (12)$$

where  $I$  represents the instantaneous rainfall intensity (mm/min).

Similarly, the design depth of a LID device ( $H^*$ ) can be expressed as:

$$H^* = \int_0^t \frac{(Q_{in} - Q_{inf})}{A_{LID}} dt \quad (13)$$

The overflow volume can be computed as:

$$W_{out} = \int_{t_0'}^t [I \times (\eta s + 1) - k] \times A_{LID} dt \quad (14)$$

Based on a drainage area (DA) and surface area (SA) ratio of 20:1 and a runoff coefficient of 0.9, a FORTRAN program was written to calculate water balance in rain garden under different storms. A flowchart for the program is presented in Figure 3.

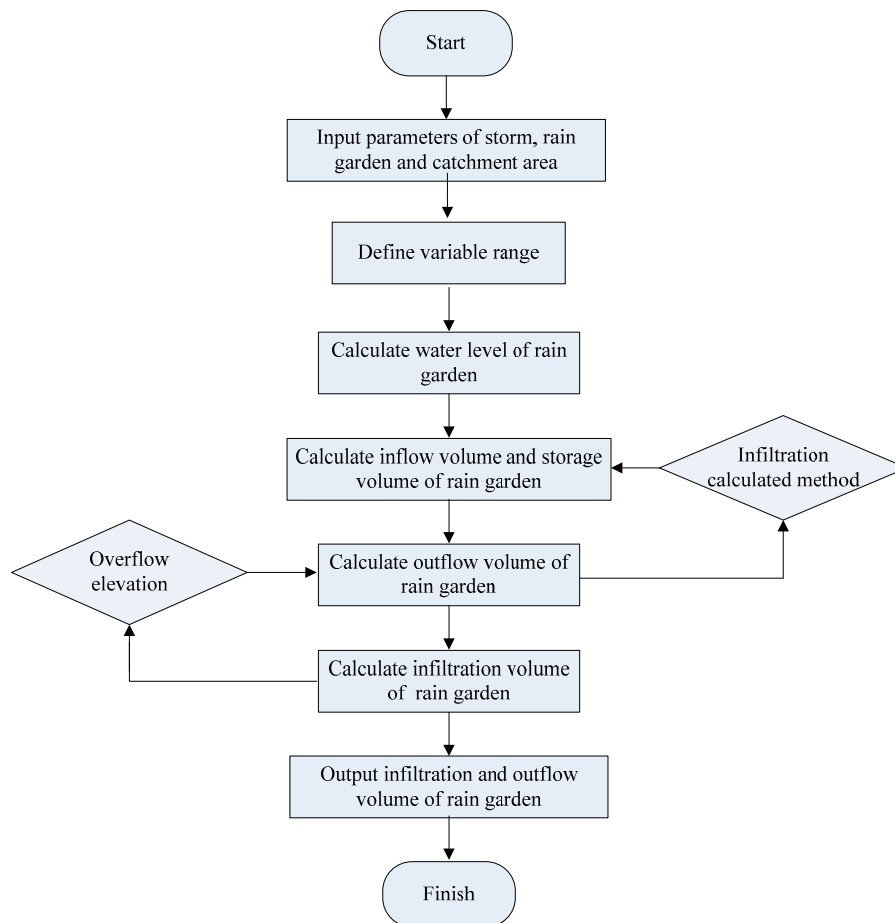


**Figure 3.** Flowchart of FORTRAN program used to calculate water balance in a rain garden (RG) under different storms.

### 2.3. Evaluation Method

After calculating designed depth ( $H$ ) and outflow volume ( $W_{out}$ ) of a LID device using the two storm representation methods as stated above, the relative differences using IDF in design depth and overflow volume may be calculated as:

$$\varphi = \frac{(H_1 - H_2)}{H_1} \times 100\% \quad (15)$$

$$\varepsilon = \frac{(W_{out1} - W_{out2})}{W_{out1}} \times 100\% \quad (16)$$

where  $H_1$  and  $H_2$  are the design depth (cm) calculated with the IDF and NDR methods, respectively, and  $W_{out1}$  and  $W_{out2}$  are the outflow volumes (mm) calculated with the IDF and NDR methods, respectively.

## 3. Results and Discussion

### 3.1. Errors in Rain Garden Design Depth Using IDF Method

The effect of rainfall processes on LID device sizing was tested. The variables included storm recurrence intervals of two years, five years, and 20 years, and storm durations of 30 min and 120 min.

Three sites with different climatic conditions were selected: (1) Nanjing located in a humid region with an annual rainfall of 1053 mm, (2) Xi'an located in a semi-humid region with an annual rainfall of 572 mm, and (3) Urumqi situated in an arid region with an annual rainfall of 282 mm. All calculations were based on a DA/SA ratio of 20 and the runoff coefficient of 0.9. The soil texture in urban greening land is mostly sandy loam or sandy soil, which has a relatively good infiltration performance, therefore, the RG soil was assumed to have a moderate infiltration rate of 1.5 m/d.

As shown in Table 2, for the design storm with 2-year recurrence interval and 30 min duration in Nanjing, when  $\sigma$  was 2, 3, and 5, the calculated design depth of the LID device was 0.57, 0.57, and 0.56 m, respectively. For the 2-year recurrence interval and 120 min duration storm, when  $\sigma$  was 2, 3, 5, the calculated design depth of LID device was 0.90, 0.89, and 0.88 m, respectively. For more intense storm events with 5-year and 20-year storms, there is little change in the calculated design depth of the LID device when  $\sigma$  is changed from 2 to 3 to 5. The different of calculated design depths for Xi'an and Urumqi were approximately the same as that for Nanjing. Considering different storm recurrence intervals and durations, the absolute differences in the design depth were within 3 cm with changes in standard deviation ( $\sigma$ ). In general, the different standard deviations of the NDR had little influence on the RG design depth. Therefore, a value of  $\sigma = 3$  was adopted to conduct the following analysis.

**Table 2.** Calculated design depth of LID device using NDR with different recurrence intervals.

Recurrence Interval (Year)	Rainfall Duration (Min)	Design Depth of NDR Intensity (m)								
		$\sigma = 2$			$\sigma = 3$			$\sigma = 5$		
		Nanjing	Xi'an	Urumqi	Nanjing	Xi'an	Urumqi	Nanjing	Xi'an	Urumqi
2	30	0.57	0.34	0.06	0.57	0.33	0.06	0.56	0.33	0.06
	120	0.90	0.43	0.08	0.89	0.42	0.06	0.88	0.42	0.04
5	30	0.72	0.47	0.09	0.71	0.47	0.08	0.70	0.47	0.08
	120	1.13	0.64	0.12	1.12	0.62	0.09	1.12	0.62	0.08
20	30	0.94	0.68	0.12	0.93	0.68	0.11	0.92	0.67	0.11
	120	1.50	0.95	0.17	1.50	0.93	0.15	1.49	0.93	0.14

The recommended design standard of rainwater utilization system is 2-year recurrence interval. For a design storm with a 2-year recurrence interval and 120 min duration, the relative difference in the design depth was calculated using the IDF and the NDR, and the relative differences under different climatic conditions were plotted in Figure 4.

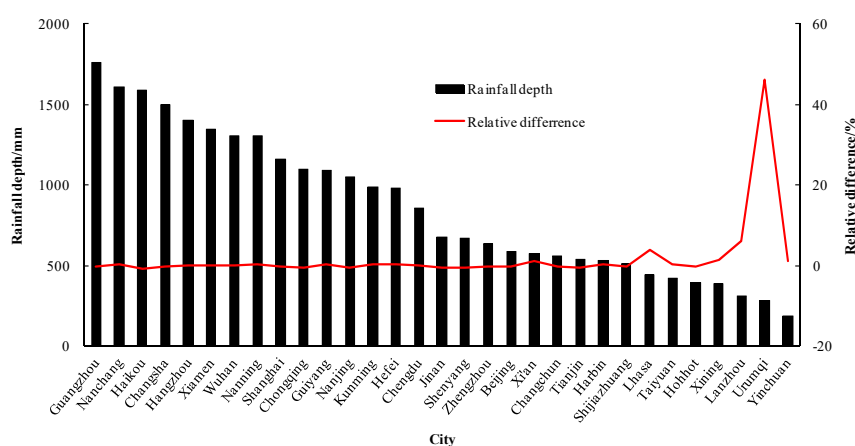


**Figure 4.** Relative differences in rain garden (RG) design depth for different cities in China, while using IDF and NDR methods when  $\sigma = 3$  (DA/SA = 20:1, runoff coefficient was 0.9 for impervious surface and infiltration rate was 1.5 m/d).

The positive values for the relative differences in Figure 4 indicate that the RG design depths using NDR were bigger than that using IDF, and vice versa. For humid regions with annual rainfall depth

greater than 800 mm, the relative differences of design depth using IDF rainfall intensity ranged from  $-0.74\%$  to  $0.33\%$ . In semi-humid areas with annual rainfall depth ranging from 400 mm to 800 mm, the relative differences were between  $-0.61\%$  and  $3.97\%$ . While in the semi-arid and arid areas with annual rainfall depth less than 400 mm, the relative differences ranged from  $-0.18\%$  to  $46.13\%$ . The biggest relative difference in design depth was  $46.13\%$  in Urumqi, but the absolute difference was just 2.8 cm. The absolute differences in design depth for 29 out of the 31 regions were within 1 cm, which related to  $94\%$  of all the selected regions. The relative differences in design depths for arid areas were greater than that for humid and semi-humid areas. These results show that, in general, the rainfall process has little influence on the design depth of the LID device under different climate conditions throughout the nation.

The reason for these errors between the two methods can be illustrated in Figure 5, which shows the real-time input and output intensity in the RG under the NDR and IDF rainfall distribution in Nanjing. Before the water level in the RG reaches the design depth, the water balance in the RG only includes inflow as an input item and infiltration as an output item.

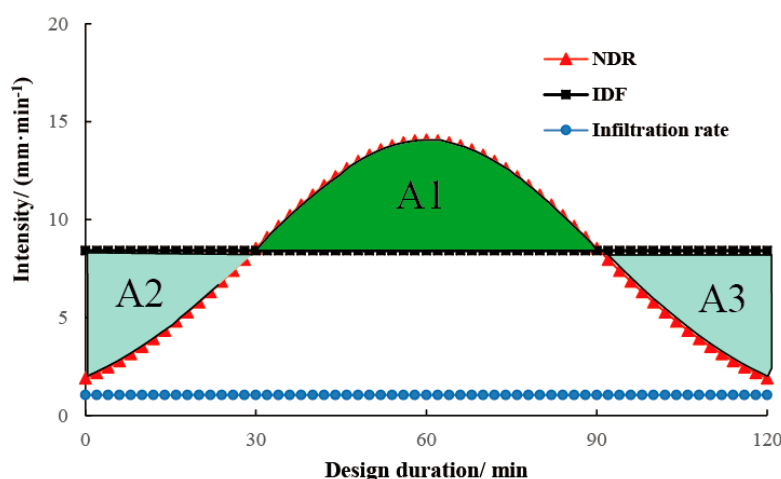


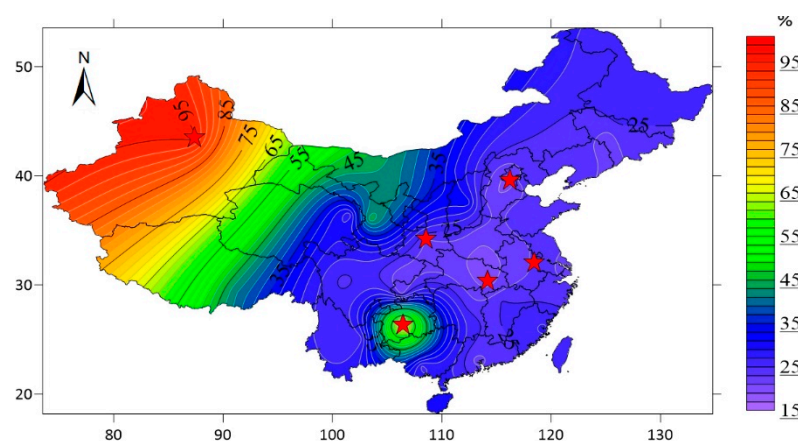
**Figure 5.** Comparison of instant intensity of RG using NDR and IDF under a 2-year design storm in Nanjing, Jiangsu, China, with a catchment area ratio of 20, runoff coefficient of 0.9, infiltration rate of 1.5 m/d, and standard deviation ( $\sigma$ ) of normal distribution of 3.

All input and output intensities were expressed by the depth of the RG area per unit time. The catchment area ratio was 20, runoff coefficient was 0.9, infiltration rate was 1.5 m/d, and the standard deviation ( $\sigma$ ) of the normal distribution was 3. Combined with the catchment area ratio, the minimum input intensity of NDR was 1.90 mm/min at the initial and final moments, and the maximum intensity was 14.07 mm/min. The input intensity with the IDF was always 8.42 mm/min. As the only output item, the infiltration rate was constant with 1.04 mm/min (1.5 m/d), and the input term was always larger than the output term throughout the entire design rainfall duration. The ponding depth of the RG reached a maximum value at the end of the design rainfall duration, which was the design depth of the RG under the corresponding design standard. The net rainfall in the RG with the NDR firstly increased and then decreased, while that with the IDF was constant throughout the entire rainfall process duration. The rainfall process integral over design duration was the total inflow volume. In this paper, the NDR processes were derived from the value of IDF. Although the actual rainfall processes with the NDR and IDF were different, the total rainfall volumes within the duration of the designed rainfall were equal. As shown in Figure 5, the area of A1 was equal to the sum of the areas of A2 plus A3. Thus, there is an insignificant difference between the design depths when using the IDF and NDR. Therefore, if the infiltration rate is always smaller than the rainfall intensity, different rainfall processes will have no influence on the design depth of the RG.

Design depth of an RG is normally determined on the basis of the plant's resistance to water submergence, which is approximately 20–30 cm. For the design storm with a 2-year recurrence interval and a 120 min rainfall duration, when the catchment area ratio is 20, the design depth calculated by the program is only four regions within the recommended range. In particular, using the proposed FORTRAN program, Haikou with the heaviest rainfall of China is calculated with a design depth of 139 cm, which is obviously unreasonable. Therefore, regions with intense rainfall intensities in southern China, when sizing the LID parameters, the catchment area ratio of the LID device can be reasonably adjusted. So that final design parameters are within the reasonable scope of the recommendations. The standard deviation ( $\sigma$ ) represents the instantaneous peak value of the rainfall intensity. These results may indicate that the effect of total volume on the design depth is more significant than the instantaneous peak rainfall intensity. However, when natural differences are considered, such as rainfall characteristics, soil properties, and other factors, the calculated deviation caused by the rainfall processes is acceptable. Thus the IDF method, which is more simple and convenient, could be adopted in the design of the LID device.

### 3.2. Error in Rain Garden Overflow Volume Using IDF Method

Overflow in the RG can occur under intense storms, and the overflow volume directly affects the runoff reduction. For storms larger than the design storm with a 2-year recurrence interval and duration of 120-min, the calculated overflow was found to vary greatly across the analyzed cities. The relative differences in overflow volumes using IDF method under a 5-year storm and 20-year storm were shown in Figure 6.



(a) 5-year recurrence interval

Figure 6. Cont.

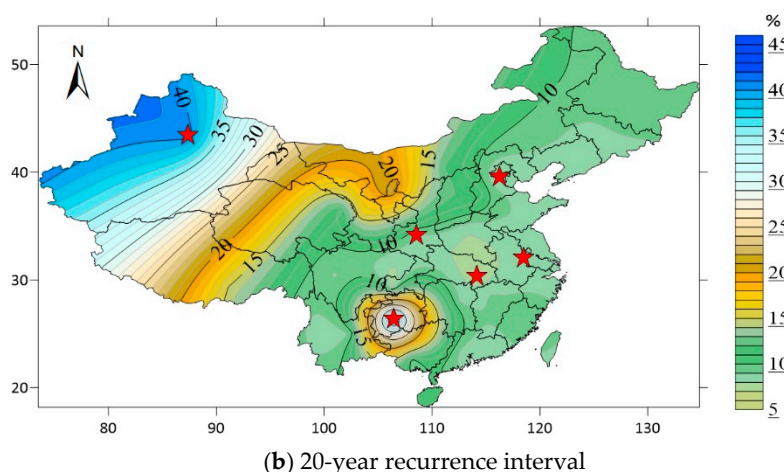


**Figure 6.** Relative difference in overflow volumes using IDF method for different cities in continental China under (a) 5-year storm and (b) 20-year storm. (DA/SA = 20:1, design depth = 25 cm and infiltration rate = 1.5 m/d based on 2-year design storm) (★ marks locations of demo cities: (from west to east) Urumqi, Guiyang, Xi'an, Wuhan, Beijing, and Nanjing).

As shown in Figure 6, for the 5-year storm, the relative differences in calculated overflow volume using IDF method ranged from 19.8% to 95.3%, and the relative differences in overflow volumes nationwide were mainly between 20% and 40% for 84% of all selected cities. While those differences for the 20-year storm ranged from 7.4% to 40.5%, and the relative differences in overflow volumes were less than 20% in 90% of all the cities nationwide. The relatively differences in overflow volume nationwide facing the 5-year storm were larger than that in the 20-year. For the 5-year storm, the correlation coefficient between the relative difference in overflow volume and the mean rainfall intensity was  $-0.60$ , and that for the 20-year storm was  $-0.61$ . For both the 5-year and 20-year storms, the biggest relative difference in overflows volume using IDF method was found in Urumqi, the smallest with the 5-year storm was 19.8% in Beijing, and that under the 20-year storm was 7.4% in Wuhan. The relative difference in overflow volumes showed a decreasing tendency from northwest to southeast. However, Guiyang was an exception, for the 5-year and 20-year storms, the relative differences in overflow volumes using IDF method were 69.3% and 39.9%. This sudden and large relative difference for the overflow in Guiyang was not in agreement with the trend of overall change, and this is attributed to the particular rainfall characteristics in Guiyang.

Figure 7 shows the ratio of mean rainfall intensity at different recurrence interval over rainfall intensity of 2-year recurrence interval in different climatic areas. No matter the 5-year, 10-year, 20-year, and 50-year rainfall recurrence interval, the intensity ratio increased from humid to arid areas. For 20-year storm, the minimum ratio is 1.2 in all humid regions, the average ratio is 1.5, and the maximum ratio is 1.7, whereas, in arid and sub-arid areas, the minimum, average, and maximum ratios are 1.7, 1.8, and 2.0 respectively. The relative difference in the overflow volume is negatively correlated with the ratio of rainfall intensity. The correlation coefficient is  $-0.90$  in humid areas and  $-0.61$  in arid areas. Although the humid areas have a deep rainfall depth, the distribution of rainfall at different frequencies is relatively concentrated, and the differences in the rainfall intensity at different frequencies are relatively small, which results in only relatively small differences in overflow volumes using IDF method. In contrast, in arid and semi-arid regions with a relatively shallow rainfall depth, the rainfall intensity distribution is dispersed throughout the different frequencies, and this results in a relatively large difference in overflow volumes using IDF method.

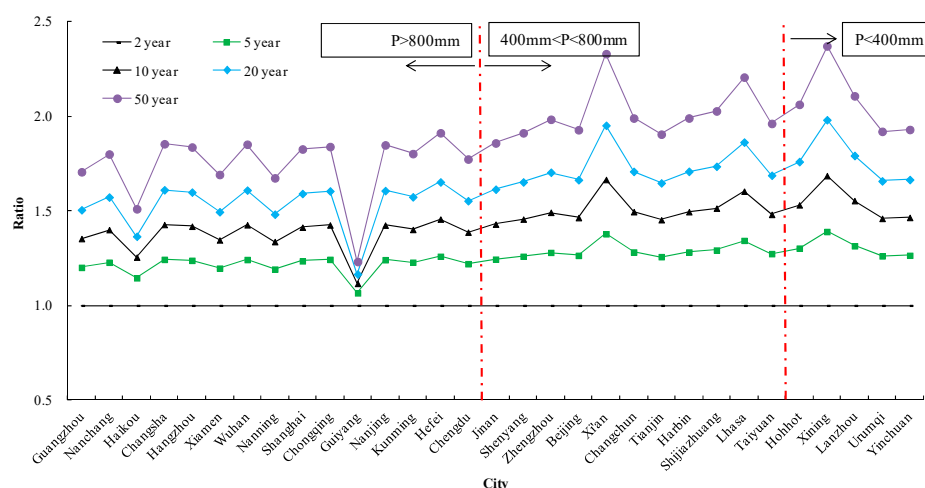


**Figure 7.** Ratio of rainfall intensity at different recurrence interval over rainfall intensity of 2-year recurrence interval in different climatic areas.

Figure 6 showed that Guiyang was contrary to the trend of the overall change. With both 5-year and 20-year storms, the relative differences in overflow volumes using IDF method are larger than those for the surrounding cities, which again conflicts with the overall change trend. Guiyang is located in a humid area with a rainfall depth greater than 800 mm. Figure 7 shows intensity ratios of 1.07, 1.12, 1.17, and 1.23 for Guiyang at the 5-year, 10-year, 20-year, and 50-year, respectively. The rainfall distribution characteristics at different frequencies in Guiyang are more concentrated and significantly different from those in the surrounding cities. Therefore, if a LID device storm was faced with storms of greater intensities, the absolute overflow volume produced would be small. In Guiyang, the overflow volume was only 0.11 cm for a storm with a 5-year recurrence interval, which shows that there is a relatively large difference of 69.3% using the IDF method.

The overall runoff reduction under the NDR method is larger than that using the IDF method nationwide. When facing a 5-year storm, the biggest difference in the runoff reduction is 5.2% in Lhasa, while the smallest is 0.8% in Guiyang. For a 20-year storm, the biggest difference is 6.8% in Urumqi and the smallest is 2.4% in Guangzhou. Therefore, the different NDR and IDF rainfall processes have a certain impact on overflow volume and runoff reduction. The average relative difference in the overflow volume is 29.9% under a 5-year recurrence interval and 12.0% under a 20-year recurrence interval. Furthermore, the average overall runoff reduction difference under the two rainfall processes is 3.4% for the 5-year storm and 3.3% for the 20-year storm. These results show that the influence of rainfall distribution on overflow estimation is greater than that on sizing the LID device.

#### 4. Conclusions

Based on the water balance in an RG/LID device, an analytical model was programmed for use in analyzing the impact of different rainfall distributions on the design parameters and the overflow estimation of LID devices. The NDR with different standard deviations ( $\sigma$ ) was used to represent different rainfall distributions when considering variable rainfall intensities during a storm process. The results indicate that the different standard deviations of the NDR had little influence on the RG design depth. Compared with the NDR method, the relative difference of design depths using IDF method in arid areas was greater than that in humid and sub-humid areas. The relative difference in 80% of the selected areas was less than 1%, and the absolute difference between the design depths in 29 out of 31 regions was within 1 cm. Overall, there was little difference in the design depth of the LID device when using IDF method. The recommended design storm of LID device by the technical guidance of sponge city construction is 2-year recurrence interval and 120 min duration. When considering storms with a greater intensity, for a 5-year storm, the relative differences in overflow

volumes nationwide using IDF rainfall intensities ranged from 19.8% to 95.3%, while those for storms with a 20-year storm ranged from 7.4% to 40.5%. The impact of rainfall distribution on the overflow volume was larger than that of the design depth.

When considering natural differences such as rainfall characteristics, soil properties, and other factors, the IDF method is acceptable for use during LID devices design. Different storm distributions were found to have little influence on design depth calculations nationwide. When LID devices are popularized in the future, it is considered that the IDF method can be used in its design. The storm intensity can be accurately calculated based on different design standards, and the design parameters can be determined according to the designed storm intensity. However, when evaluating the performance of existing LID devices, it is necessary to employ accurate rainfall process data.

**Author Contributions:** Conceptualization, S.T., Q.X., and Z.J.; Methodology, S.T., Q.X., Z.J., and W.L.; Simulation, S.T., Q.X., and Z.S.; Writing review and editing, S.T., Z.J., and W.L.

**Funding:** Funding for this research was partially supported by the Natural Science Foundation of Jiangsu Province (Grant No. BK20170504) and the Priority Academic Program Development of Jiangsu Higher Education Institutions (PAPD).

**Conflicts of Interest:** The authors declare no conflicts of interest.

## References

1. Dietz, M.E.; Clausen, J.C. Stormwater runoff and export changes with development in a traditional and low impact subdivision. *J. Environ. Manag.* **2008**, *87*, 560–566. [[CrossRef](#)] [[PubMed](#)]
2. Xu, C.Q.; Hong, J.L.; Jia, H.F.; Liang, S.D.; Xu, T. Life cycle environmental and economic assessment of a LID-BMP treatment train system: A case study in China. *J. Clean. Prod.* **2017**, *149*, 227–237. [[CrossRef](#)]
3. Qiao, X.J.; Kristoffersson, A.; Randrup, T.B. Challenges to implementing urban sustainable stormwater management from a governance perspective: A literature review. *J. Clean. Prod.* **2018**, *196*, 943–952. [[CrossRef](#)]
4. Lucke, T.; Nichols, P.W.B. The pollution removal and stormwater reduction performance of street-side bioretention basins after ten years in operation. *Sci. Total Environ.* **2015**, *536*, 784–792. [[CrossRef](#)] [[PubMed](#)]
5. China Ministry of Housing and Urban-Rural Construction (CMHURC). *Technical Guidelines on Sponge City Construction—Low Impact Development Stormwater Management System*; CMHURC: Beijing, China, 2014.
6. Jiang, Y.; Zevenbergen, C.; Ma, Y.C. Urban pluvial flooding and stormwater management: A contemporary review of China's challenges and "sponge cities" strategy. *Environ. Sci. Policy* **2018**, *80*, 132–143. [[CrossRef](#)]
7. Li, L.Q.; Davis, A.P. Urban Stormwater Runoff Nitrogen Composition and Fate in Bioretention Systems. *Environ. Sci. Technol.* **2014**, *48*, 3403–3410. [[CrossRef](#)]
8. Chui, T.F.M.; Liu, X.; Zhan, W. Assessing cost-effectiveness of specific LID practice designs in response to large storm events. *J. Hydrol.* **2016**, *533*, 353–364. [[CrossRef](#)]
9. Zahmatkesh, Z.; Burian, S.J.; Karamouz, M.; Tavakol-Davani, H.; Goharian, E. Low-Impact Development Practices to Mitigate Climate Change Effects on Urban Stormwater Runoff: Case Study of New York City. *J. Irrig. Drain. Eng.* **2015**, *141*, 04014043. [[CrossRef](#)]
10. Zeng, S.Y.; Guo, H.; Dong, X. Understanding the synergistic effect between LID facility and drainage network: With a comprehensive perspective. *J. Environ. Manag.* **2019**, *246*, 849–859. [[CrossRef](#)]
11. Chen, Z.H.; Yin, L.; Chen, X.H.; Wei, S.; Zhu, Z.H. Research on the characteristics of urban rainstorm pattern in the humid area of Southern China: A case study of Guangzhou City. *Int. J. Climatol.* **2015**, *35*, 4370–4386. [[CrossRef](#)]
12. Liu, C.Y.; Chui, T.F.M. Factors Influencing Stormwater Mitigation in Permeable Pavement. *Water* **2017**, *9*, 988.
13. Tung, Y.K. Uncertainty analysis and risk-based design of detention basin without damage function. *Water Resour. Res.* **2017**, *53*, 3576–3598. [[CrossRef](#)]
14. Cording, A.; Hurley, S.; Whitney, D. Monitoring Methods and Designs for Evaluating Bioretention Performance. *J. Environ. Eng.* **2017**, *143*, 05017006. [[CrossRef](#)]
15. Balbastre-Soldevila, R.; García-Bartual, R.; Andrés-Doménech, I. A Comparison of Design Storms for Urban Drainage System Applications. *Water* **2019**, *11*, 757. [[CrossRef](#)]

16. Hailegeorgis, T.T.; Alfredsen, K. Analyses of extreme precipitation and runoff events including uncertainties and reliability in design and management of urban water infrastructure. *J. Hydrol.* **2017**, *544*, 290–305. [\[CrossRef\]](#)
17. Jia, Z.H.; Tang, S.C.; Luo, W.; Li, S.; Zhou, M. Small scale green infrastructure design to meet different urban hydrological criteria. *J. Environ. Manag.* **2016**, *171*, 92–100. [\[CrossRef\]](#) [\[PubMed\]](#)
18. Li, J.K.; Deng, C.N.; Li, H.E.; Ma, M.H.; Li, Y.J. Hydrological Environmental Responses of LID and Approach for Rainfall Pattern Selection in Precipitation Data-Lacked Region. *Water Resour. Manag.* **2018**, *32*, 3271–3284. [\[CrossRef\]](#)
19. Nguyen, V.T.; Desramaut, N.; Nguyen, T.D. Optimal rainfall temporal patterns for urban drainage design in the context of climate change. *Water Sci. Technol.* **2010**, *62*, 1170–1176. [\[CrossRef\]](#)
20. Cen, G.P.; Shen, J.; Fan, R.S. Research on rainfall pattern of urban design storm. *Adv. Water Sci.* **1998**, *9*, 41–46. (In Chinese)
21. Griffis, V.W.; Stedinger, J.R. Log-Pearson type 3 distribution and its application in flood frequency analysis (II): Parameter estimation methods. *J. Hydrol. Eng.* **2007**, *12*, 492–500. [\[CrossRef\]](#)
22. Huff, F.A. Time distribution of rainfall in heavy storms. *Water Resour. Res.* **1967**, *3*, 1007–1019. [\[CrossRef\]](#)
23. Khatavkar, P.; Mays, L.W. Optimization Models for the Design of Vegetative Filter Strips for Stormwater Runoff and Sediment Control. *Water Resour. Manag.* **2017**, *31*, 2545–2560. [\[CrossRef\]](#)
24. Chin, D.A. Designing Bioretention Areas for Stormwater Management. *Environ. Process.* **2017**, *4*, 1–13. [\[CrossRef\]](#)
25. Kurtz, T. Managing Street Runoff with Green Streets. In *Low Impact Development for Urban Ecosystem and Habitat Protection*; ASCE: Reston, VA, USA, 2009; pp. 1–10.
26. Rubinato, M.; Shucksmith, J.; Saul, A.J.; Shepherd, W. Comparison between Info Works hydraulic results and a physical model of an urban drainage system. *Water Sci. Technol.* **2013**, *68*, 372–379. [\[CrossRef\]](#) [\[PubMed\]](#)
27. Xie, J.Q.; Chen, H.; Liao, Z.L.; Gu, X.Y.; Zhu, D.J.; Zhang, J. An integrated assessment of urban flooding mitigation strategies for robust decision making. *Environ. Model. Softw.* **2017**, *95*, 143–155. [\[CrossRef\]](#)
28. Rosa, D.J.; Clausen, J.C.; Dietz, M.E. Calibration and verification of SWMM for low impact development. *J. Am. Water Resour. Assoc.* **2015**, *51*, 746–757. [\[CrossRef\]](#)
29. Gao, J.; Wang, R.S.; Huang, J.L.; Liu, M. Application of BMP to urban runoff control using SUSTAIN model: Case study in an industrial area. *Ecol. Model.* **2015**, *318*, 177–183. [\[CrossRef\]](#)
30. Brown, R.A.; Skaggs, R.W.; Hunt, W.F. Calibration and validation of DRAINMOD to model bioretention hydrology. *J. Hydrol.* **2013**, *486*, 430–442. [\[CrossRef\]](#)
31. Mailhot, A.; Duchesne, S. Design Criteria of Urban Drainage Infrastructures under Climate Change. *J. Water Resour. Plan. Manag.* **2010**, *136*, 201–208. [\[CrossRef\]](#)
32. Tang, S.C.; Luo, W.; Jia, Z.H.; Liu, W.L.; Li, S.; Wu, Y. Evaluating retention capacity of infiltration rain gardens and their potential effect on urban stormwater management in the sub-humid loess region of China. *Water Resour. Manag.* **2016**, *30*, 983–1000. [\[CrossRef\]](#)
33. Davis, A.P.; Traver, R.G.; Hunt, W.F.; Lee, R.; Brown, R.A.; Olszewsk, J.M. Hydrologic performance of bioretention storm-water control measures. *J. Hydrol. Eng.* **2011**, *17*, 604–614. [\[CrossRef\]](#)
34. Hunt, W.F.; Davis, A.P.; Traver, R.G. Meeting hydrologic and water quality goals through targeted bioretention design. *J. Environ. Eng.* **2012**, *138*, 698–707. [\[CrossRef\]](#)
35. Xia, J.; Zhang, Y.Y.; Xiong, L.H.; He, S.; Wang, L.F.; Yu, Z.B. Opportunities and challenges of Sponge City construction related to urban water issues in China. *Sci. China Earth Sci.* **2017**, *60*, 652–658. [\[CrossRef\]](#)
36. China Ministry of Housing and Urban-Rural Construction (CMHURC). *National Urban Storm Intensity Formula Catalogue*; CMHURC: Beijing, China, 2014.
37. Liu, S.S.; Bai, M.J.; Xu, D.; Li, Y.N.; Hu, W.D. Parameters simplification of Green-Ampt infiltration models and relationships between infiltration and soil physical parameters. *Trans. CSAE* **2012**, *28*, 106–110. (In Chinese)

